Iranian Journal of Chemical Engineering
Vol. 11, No. 1 (Winter), 2014, IAChE

Effect of Amino Acids on Magnesium Ammonium Phosphate Hexahydrate (Struvite) Crystallization

S. Titiz-Sargut, P. Sayan, A. Masum, B. Kiran*
Marmara University, Faculty of Engineering, Chemical Engineering Department, Goztepe Campus, Istanbul-Turkey

Abstract

Struvite crystallization was investigated in the presence of different amino acids at 37°C and pH 8.0 in a continuous crystallization system. Crystal size distributions, filtration rates and morphologies of struvite crystals were determined and discussed as a function of amino acid concentration. The change of morphology depending on the amino acid type and concentration affected the filtration characteristics of struvite crystals. The crystal size distributions of the final products obtained at investigated experimental conditions were evaluated by using modified form of Abegg, Stevens and Larson (ASL) model. Thermogravimetric and differential thermal analysis have been used for thermal characterization of struvite crystals by measuring the changes in their physicochemical properties as a function of increasing temperature with time. The Coats-Redfern integral method was used to evaluate the kinetic parameters in the decomposition sequence observed in the TGA curves. In the presence of all investigated amino acids, the form of precipitate was struvite and newberyite formation was not observed.

Keywords: *Struvite, Amino Acids, Size Dependent Growth, ASL Model, Coats-Redfern Method*

1. Introduction

Struvite ($MgNH_4PO_4.6H_2O$) precipitates as stable white orthorhombic crystals in a 1:1:1 molar ratio according to Eq(1) (with n=0,1 and 2 as a function of pH) [1]:

$$Mg^{2+} + NH_4^+ + H_nPO_4^{n-3} + 6H_2O \rightarrow MgNH_4PO_4 6H_2O + nH^+ \quad (1)$$

The major reaction product has always been identified as the hexahydrate, struvite ($MgNH_4PO_4.6H_2O$). However, lower hydrates, namely the monohydrate, dittmarite ($MgNH_4PO_4.H_2O$) and the tetrahydrate scherlite [$(NH4)_2MgH_2(PO_4)_2.4H_2O$] have also been identified in these systems in small quantities. Dittmarite and/or scherlite have been postulated to form as intermediate reaction products before they transform to the more stable hexahydrate, struvite.

* Corresponding author: perviz.sayan@marmara.edu.tr

Struvite ($MgNH_4PO_4.6H_2O$) is also known to form a hard scale in specific areas of wastewater treatment plants such as in sludge liquors pipes, centrifuges, belt presses, and heat exchangers [2]. The mass of crystalline deposits formed can be extensive and can lead to operational failure by clogging water distribution pipes. Many studies on struvite crystallization are limited on the application oriented thermodynamics such as struvite solubility and much less on the kinetics [3]. It has been reported that the presence of impurities in solution can block or inhibit struvite crystals formation and also increase or decrease the crystal size [3]. In literature, it has been reported that the presence of sodium, calcium, sulphate and carbonate ions affected the induction time, struvite crystal morphology and sizes [4].

Struvite is also one of the stones in the urinary tract which is seen in human and animals. It compromises approximately 15% of urinary tract stones seen in humans, 88% in cats and 70 % in dogs. The formation of the other urinary tract infections stones like struvite is frequently initiated by urea reduced with urease of proteus bacteria. A variety of substances contained in the urine have been described as crystallization–inhibitor molecules, some of them of low molecular weight such as magnesium citrate, some amino acids and others with high molecular weight such as glycosaminoglycans, Tamm-Horsfall glycoprotein, nephrocalcin and osteopontin [5-7]. Many organic constituents in urine, including proteins, have surfactant properties. Among other organic molecules, urine contains biological surfactants, bile salts, which are responsible for lowering urinary surface tension and have a potential inhibitory role in urinary stone development [8]. Proteins are composed of subunits called amino acids. Amino acids have both an amine and a carboxylic acid functional group and are therefore both acid and base at the same time [9]. Amino acids are also important in many other biological molecules, such as forming parts of co-enzymes, as in S-adenosylmethionine, or as precursors for the biosynthesis of molecules such as heme. As a result of their central role in biochemistry, amino acids are very important in nutrition. When taken up into the body in the diet, the twenty standard amino acids are either used to synthesize proteins and other biomolecules or oxidized to urea and carbon dioxide as a source of energy [10]. Of the twenty standard amino acids, eight are called essential amino acids because the human body cannot synthesize them from other compounds at the level needed for normal growth, so they must be obtained from food [11]. It has also been reported that the physical and chemical properties of amino acids are very important in terms of being not only the basic building blocks of proteins and peptides but also for their importance in industrial processes, particularly in pharmaceutical and crystallization processes [12]. Amino acids contain chiral carbon atoms directing the crystallization in noncentrosymmetric space group and also possess zwitterion nature favoring crystal hardness [13,14]. The addition of amino acids in the semi organic material like potassium acid phthalate may perform modification or changes in the lattices or crystal behaviors. Elakkina

Kumaran *et al*. have investigated the effect of L-alanine, glycine and L-tyrosine on the growth, morphology, structural, optical, thermal and mechanical properties of potassium acid phthalate crystals. Koutsopoulos and Dalas have also investigated the interaction of acidic amino acids with hydroxyapatite in order to assess their effect on crystal growth and elucidate the mechanism of action [15]. They have reported that aspartic and glutamic acid decreased the growth rates of hydroxyapatite markedly and amino acids' action is due to adsorption and subsequent blocking of the active growth sites onto the surface of the hydroxyapatite crystals. The influence of aliphatic amines, diamines and amino acids on the polymorph of calcium carbonate was investigated by Wittaya Chuajiw *et al* [16]. They have reported that amino acids additives played an important role in the phase transformation of calcium carbonate. Most reports suggested that the major factor for controlling the crystal shape was the accessibility of the amino groups to the calcium carbonate crystal surfaces [17-20]. Based on the above arguments, the present work investigates the effect of amino acids on struvite crystallization kinetics and morphology with the intention of gaining a better understanding of struvite formation and prevention in urinary system.

2. Materials and methods

The set of experiments was conducted using synthetic solution made up of analytical grade $MgCl_2$ and $NH_4H_2PO_4$ purchased from Merck Company. Amino acids used in the experiments were supplied from Aldrich Company. Crystallization of struvite obtained from the reaction of pure magnesium chloride solution (10% w/w) and ammonium dihydrogen phosphate solution (10%, w/w) was carried out in the study of the laboratory scale MSMPR (Mixed Suspension Mixed Product Removal) crystallizer shown in Fig. 1.

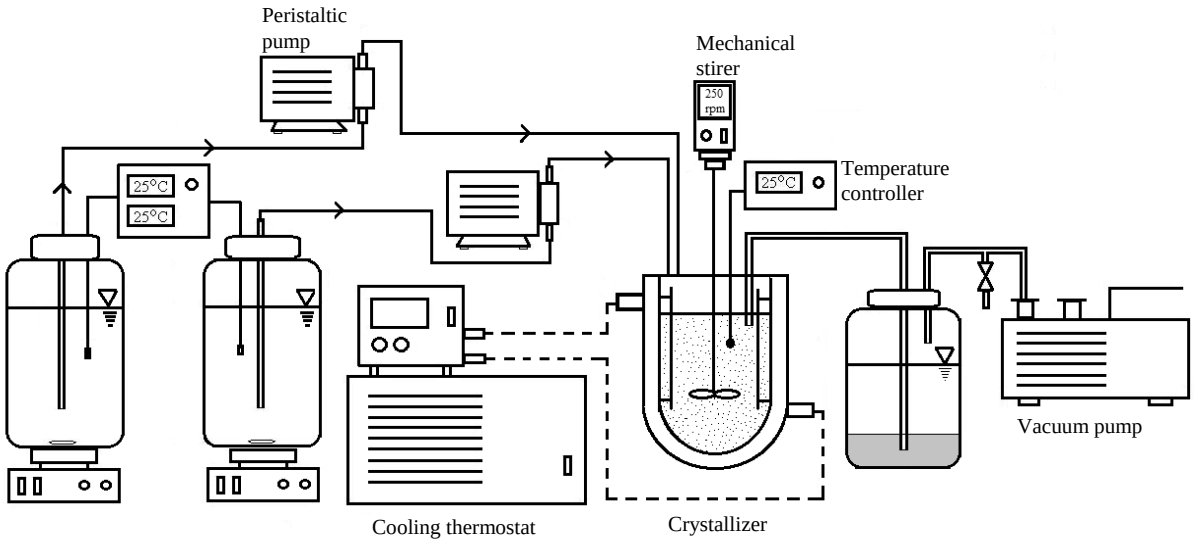

Figure 1. Experimental Set-up.

Experiments were performed in a 0.5 L jacketed glass crystallizer with a U-shaped bottom, which was equipped with a three blade impeller and three baffles. The impeller was rotated at a speed of 250 rpm to ensure all the particles were well suspended. Precise temperature control in the crystallizer was achieved by thermostat system. Stoichiometric feed solutions of reactants based on the fundamental reaction of struvite crystallization and amino acids were fed into the crystallizer by peristaltic pumps. The initial pH of reactive solution (about 5.38) was slowly brought up to saturation level using 0.5 M of NaOH and afterward 0.1 M of sodium hydroxide was slowly added until the first appearance of crystal cloud in solution. During the experiments constant pH and constant reactant concentration were employed. The system was run for a period of eight residence times in order to attain a steady state in the crystallizer. Residence time was chosen as 1 h. Then the characteristic suspension sample was withdrawn at isokinetic velocity and crystals were separated from mother liquor by vacuum filtration. Crystals were dried in air before being used for further studies. CSD was determined by laser diffraction particle size analyzer (MALVERN 2000). CSD analyses results were evaluated by using the linearized form of population balance equation to determine the kinetic parameters [21]. Dynamic filtration studies were conducted in the laboratory vacuum filtration described in detail in the literature [22]. The laboratory filtration data were used to calculate the cake parameters based on Darcy's law [23]. The inverse of time rate change of the volume of filtrate during filtration is expressed as follows:

$$\frac{d\theta}{dv} = K_p V + B \tag{2}$$

A plot of dθ/dV as the dependent variable and V as the independent variable results in a straight line where the Kp and B are the slope and intercept respectively. Kp and B are:

$$K_p = \frac{c\alpha\mu}{A^2(-\Delta p)} \tag{3}$$

$$B = \frac{R_m \mu}{A(-\Delta p)} \tag{4}$$

where c ($kg.m^{-3}$) is the concentration of the slurry, μ ($kg.m^{-1}s^{-1}$) is the viscosity of liquid, A (m^2) filter surface area, Δp ($kg.m^{-2}$) applied pressure difference for filtration, α($m.kg^{-1}$) mean specific cake resistance, R_m(m^{-1}) filter medium resistance. For characterisation struvite crystals were examined by powder X-ray diffraction (XRD-Rigaku, Japan) using Ni filtered Cu-Kα radiation and scanning rate of $2°min^{-1}$, 40 kV, 30 mA. The divergence and scattering slit was 1° for the range $5°<2\theta<60°$. FT-IR spectra were recorded with a FT-IR spectrometer Bruker Tensor 27 using KBr pellets between 4000 and 400 cm^{-1}. The reproducibility of the results was confirmed well by measuring several pellets made from a certain species. SEM was performed using JEOL 5410 LV scanning electron microscope operating at 10 kV. The struvite crystals used for SEM were air dried and sputter-coated with gold. Thermal Analysis of struvite crystals was

carried out with a thermogravimetric analyzer Netsch STA 409, in the athmosphere of air from room temperature to 900°C at a heating rate of 10°C/min.

3. Results and discussion

In order to determine the influence of amino acids on struvite precipitation, a series of experiments in the range of 0-2000 ppm amino acid concentrations at pH 8.0 and 37°C were done in a MSMPR type crystallizer. Two essential (DL-Lysine, tryptophane) and two non-essential (D(+) Proline, L- Alanine) amino acids were used in the experiments. The identification of precipitate was confirmed by infrared and XRD analysis. FT-IR spectrum and XRD pattern were given in Figs. 2 and 3 respectively. According to Fig. 2, the absorptions occurring between 3500 and 3250 cm^{-1} are due to O-H and N-H stretching vibrations. This also suggests the presence of water of hydration. The band at 1437 cm^{-1} is due to the asymmetric H-N-H bending vibration. Vibrations localized in the 1000 and 450 cm^{-1} region are characteristic of the phosphate group. The strongest peak at 1000 cm^{-1} is due to the asymmetric stretching phosphate vibration. The absorptions taking place at 769.2 and 701.6 cm^{-1} are due to rocking of N-H bond and absorption at 582 cm^{-1} may be due to metal-oxygen bond. Thus, the FT-IR spectrum proves the presence of water of hydration, N-H bond, P-O bond, NH_4^+ ion and PO_4^- ion and metal-oxygen bond. According to Figs. 2 and 3, the results are in agreement with reference data for Struvite ($MgNH_4PO_4.6H_2O$) crystals [24].

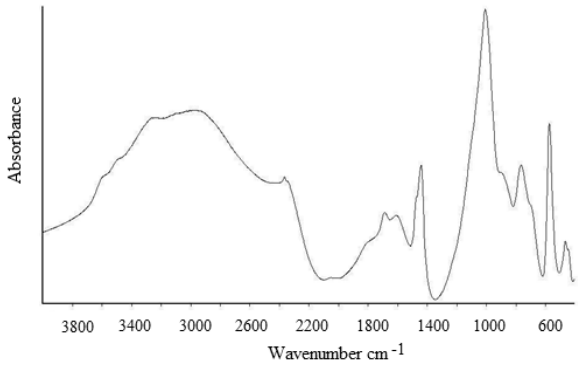

Figure 2. FT-IR spectrum of struvite crystal grown at pH 8.0 and 37°C.

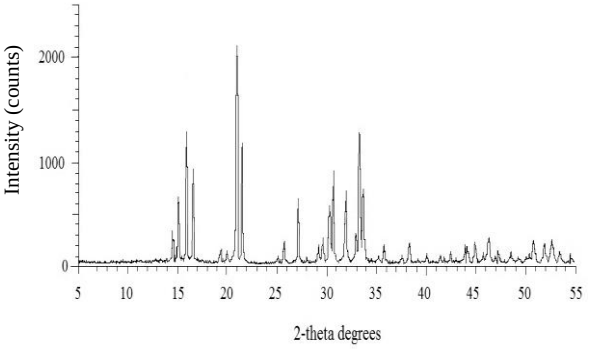

Figure 3. XRD pattern of struvite crystal grown at pH 8.0 and 37°C.

Apparent particle size (determined as 50% retained from cumulative oversize) of struvite obtained in the presence of different amino acid concentrations is shown in Fig.4. The mean volume diameter values from the instrument used in this study are reported as apparent particle size. As can be seen from Fig.4, apparent particle size of struvite increased in the range of 0-1000 ppm amino acid concentrations except in the presence of tryptophan. Increasing with amino acid concentration, the apparent particle size remained either almost constant or decreased slightly. In the presence of tryptophan, apparent particle size showed independent tendency from the amino acid

concentration and did not change compared to pure media.

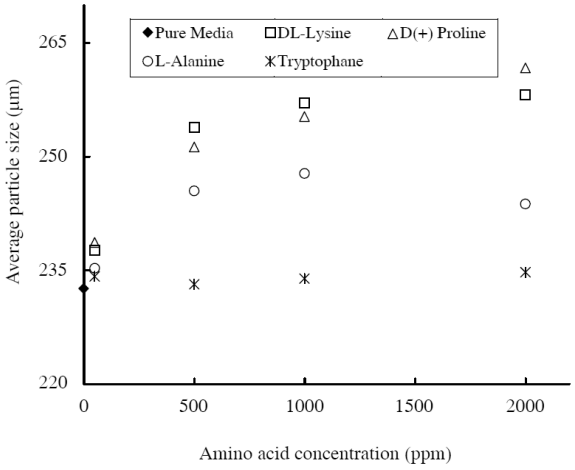

Figure 4. Change of apparent particle size of struvite grown in pure media and in the presence of different amino acid concentrations.

According to Fig. 4, the apparent particle size increased in the order: Tryptophane < D-alanine< D(+)-Proline<DL-Lysine. As mentioned in experimental procedure part, in order to determine filtration characteristics of struvite crystals in the presence of amino acids, filtration rates values were evaluated according to the general filtration equation for dilute solutions and the results were given in Fig. 5 and Table 1. As can be seen from Fig. 5, struvite crystals obtained in the presence of amino acids have lower specific cake resistance compared to pure media. Only in the presence of tryptophan, as expected, do struvite crystals have similar specific cake resistance results to pure media. Fig. 6 shows the SEM photographs of struvite crystals obtained in the presence of 1000 ppm amino acid concentrations.

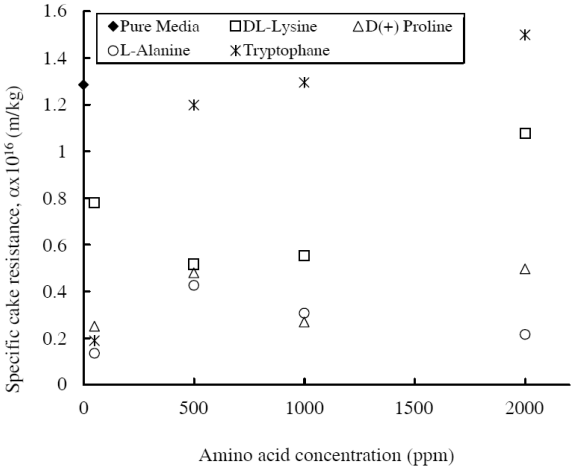

Figure 5. Comparison of specific cake resistance of struvite crystals grown in the presence of different amino acids (pH 8.0; T=37°C).

As can be seen from Fig.6, struvite crystals obtained both in pure media and in the presence of all amino acids investigated in this study, are seen as mostly aggregated or agglomerated particles.

Table 1. Filter medium resistance of struvite obtained in the presence of different concentrations of amino acids.

Amino Acid Concentration (ppm)	**Filter Medium Resistance, $R_m x10^{10}$ (m^{-1})**			
	DL-Lysine	**D(+) Proline**	**L-Alanine**	**Tryptophane**
0 (pure media)	5,162	5,162	5,162	5,162
50	4,296	3,528	4,19	3,539
500	3,788	4,01	4,399	4,583
1000	3,367	3,672	4,184	6,357
2000	4,247	2,578	5,138	5,969

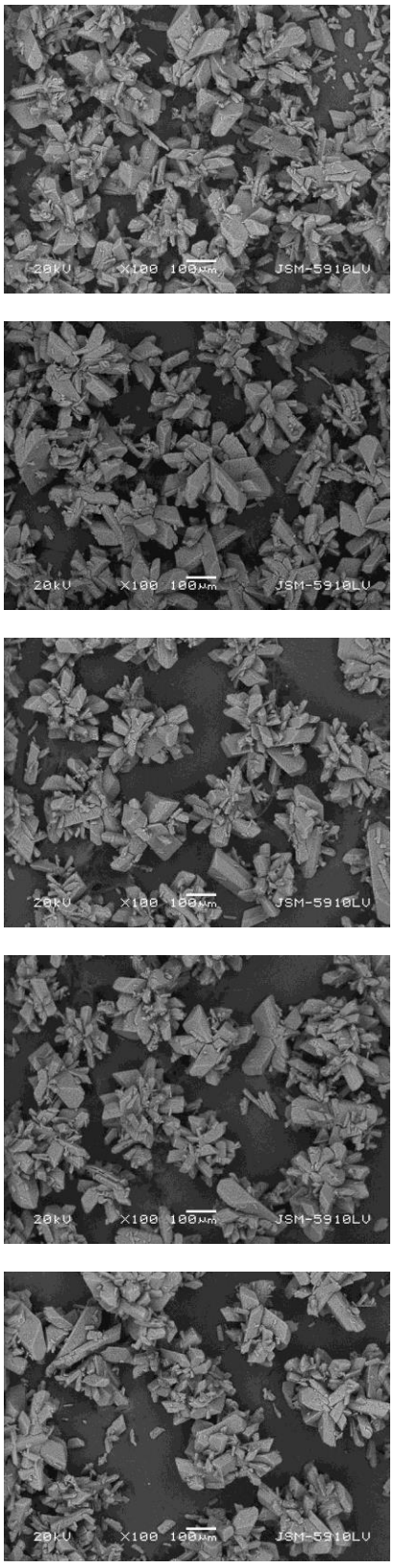

Figure 6. SEM photographs of struvite crystals grown in pure media (a) and in the presence of 1000 ppm (b) DL-Lysine (c) D(+)-Proline (d) L-Alanine (e) Tryptophane (pH 8.0; T=37°C).

Fig. 6-a shows that struvite crystals obtained in pure media are not only aggregates but also grown in the form coffin into each other. However these aggregates are not very compact, thus they can be easily broken due to hydrodynamic conditions in the crystallizer. In the presence of amino acids, struvite crystals have a similar shape to those obtained in pure media, however, the mechanical strength of aggregates or agglomerates changes depending on amino acid type and concentration. Struvite crystals obtained both in pure media and in the presence of amino acids grow mainly twin-like or triplet-like as a main structure and, further, grow as small aggregates on the growth point. It is clear that the number and mechanical strength of these small aggregates or agglomerates affect the filtration rate. Attrition rate values which describe the mechanical strength of struvite crystals were measured for 1000 ppm amino acid concentrations and were given in Table 2. Attrition rate measurements were done in a fluidized bed described in literature [25].

Table 2. Attrition rate values of struvite crystals obtained in the presence of 1000 ppm amino acid concentrations.

	Pure Media	**DL-Lysine**	**D(+) Proline**	**L-Alanine**	**Tryptophane**
Attrition rate (%)	15,2	6,0	5,2	9,1	14,0

Table 2 shows that in the presence of DL-Lysine and D(+) Proline, struvite crystals having fewer number of small aggregates or agglomerates or having high mechanical strength compared to pure media show lower specific cake resistance.

Correspondingly, as it is seen from Fig. 5, in the presence of L-Alanine, struvite crystals have higher specific cake resistance values than those obtained in the presence of DL-Lysine and D(+) Proline. As can be seen from the SEM photographs, the number of small particles on the main structure are more than those obtained in the presence of DL-Lysine and D(+) Proline. Moreover, in the presence of L-Alanine, twin-like or triplet-like forms as a main form are seldom seen. As a matter of fact, breakage of these small particles due to the fluid dynamic conditions in the crystallizer affect the filtration rate, hence the specific cake resistance is increased. In the presence of tryptophan, struvite crystals have similar specific cake resistance values with pure media. According to the SEM photographs, it is clearly seen that struvite crystals obtained in the presence of tryptophan do not have a definite shape. The majority of struvite crystals are seen as consisting of breaking particles that have come together. This indicates that the presence of tryptophan in crystallization media weakens the mechanical strength of struvite crystals. According to Table 1, the filter medium resistance values support the specific cake resistance results.

In mass crystallization processes a population balance theory was used to describe the nucleation and growth of crystals formed in the reactor. For the basic, simplified approach to the mass crystallization process kinetics, assuming steady state in a continuous crystallizer with ideally mixed content and withdrawal of a non-classified, representative product (MSMPR type crystallizer), the population balance equation can be formulated in a general form of simple differential equation [26]:

$$\frac{d(nG)}{dL}+\frac{n}{\tau}=0 \tag{5}$$

If the growth rate is size independent, i.e. Mc Cabe's ΔL law is valid,

$$n=n^{\circ}exp(-\frac{L}{G\tau}) \tag{6}$$

the crystal growth rate may be determined from the slope of semi-logarithmic population density graph while the intercept of the line gives the value of $\ln(n^{o})$. Nucleation rate can be determined as

$$B^{\circ}=n^{\circ}G \tag{7}$$

Fig. 7 shows the population density values versus crystal size of struvite crystals obtained in pure media and in the presence of 1000 ppm amino acid concentrations for τ=1 h. As it can be clearly seen from Fig. 7 the population density results for struvite crystals obtained in pure media and in the presence of 1000 ppm amino acid concentrations deviate from linearity. Greater than 90μm crystal size, deviation from the linearity may be caused by either breakage of the crystals caused by mechanical stress or agglomeration and destruction of agglomerates [27]. Thus, the shape of a population density plot does not on its own explain the particular effect that has caused the deviation in a particular experiment. As it is seen from Fig. 7, for the smallest size crystals, the population density distributions

are concave to top. This type of population density distribution can result from the occurrences of growth rate dispersion, secondary nucleation and size dependent difference in a relative fluid crystal velocity.

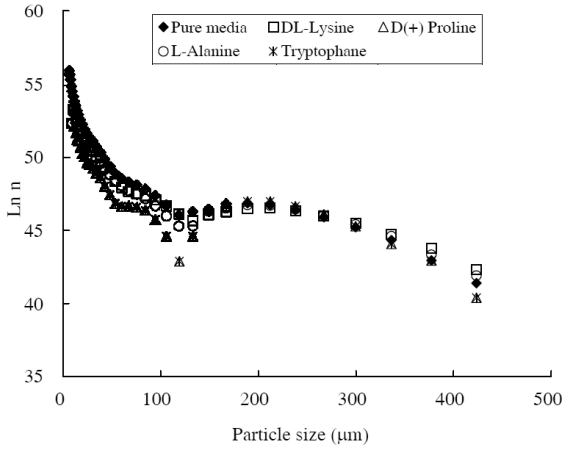

Figure 7. Population density graph of struvite crystals grown in pure media and in the presence of 1000 ppm amino acid concentrations.

However, it is impossible to distinguish between size-dependent growth on the one hand and growth dispersion on the other by analyses of MSMPR alone. In order to accommodate the concept of size-dependent growth, several empirical relationships between G and L have been proposed [28]. Theoretical analysis regarding mathematical construction of these functions proved that equations proposed in literature are valid only for the crystals of finite size [29-31]. Assumption of zero-size nucleus makes its further growth impossible from mathematical point of view. Thus, for practical application of these formulas it is necessary to assume arbitrary starting size for nucleus, the value of which can introduce some unpredictable calculation error. ASL-model proposed a solution of Eq. 2 as analytical expression $n(L)$ to comply with assumed $G(L)$ form as follow [32]:

$$G(L) = G^{\circ}(1+aL)^{b} \tag{8}$$

This empirical equation is capable of describing systems where growth rate is inversely proportional to the size of particles. On the other hand, it is difficult to find out the nuclei density when the population balance of ASL equation is used [33]. Jancic and Garside showed that extrapolation of experimental points may lead to very different results in nuclei size [34]. Results may change depending on the extrapolation method and measuring technique of particle size distribution. For the present study, ASL model was used to model size dependent growth rates for only under 90 μm crystal size range. It is important to mention that for this study ASL model would not be suitable to calculate growth rate for the crystals larger than 90 μm due to agglomeration or attrition. Therefore, larger crystals were not considered to model the size dependent growth rate. In the proposed model the smallest particle size that we could measure was selected and standardization procedure was applied. In all experiments the smallest particle size was taken as 7 μm. Under this condition the growth rate which is dependent on particle size can be written as follows:

$$G = G^{*}[1+a(L-L^{*})]^{b} \tag{9}$$

where G^* is the growth rate for particles at 7 μm average size. Substituting the growth rate G (Eq. 6) in Eq. 2 and integrating Eq. 2, the following population density equation is obtained:

$$n(L) = n[1+a(L-7)]\ exp\frac{1-(1+a(L-7)^{1-b}}{1-b} \quad (10)$$

Where $a = \frac{1}{G^*\tau}$. The growth rate of nuclei G^*, nuclei number density n^*, and exponent of size dependency b are obtained by fitting the experimental data to the above equation (Eq.7). The parameter b is usually less than 1. When b=0 model is turned to model of independent particle size. The growth rate increases with size volume and vice versa when b is positive. In this case nucleation rate can be expressed as:

$$B^* = n^*.G^* \quad (11)$$

Eq. 7 was fitted to the population density data to obtain the model parameters G^*, n^*, and b. Fig. 8 can be given as an example showing the fitted population density of struvite crystals grown in pure media for 1 h residence time.

Table 3 gives the coefficients to be used to find size dependent growth rate of struvite crystals obtained in pure media and in the presence of 1000 ppm amino acid concentrations for 1 h residence time. As can be seen from Table 3, the obtained parameter b is positive, meaning growth rate increases with size volume. The nucleation rate was calculated based on Eq. 8 and the results were also given in Table 3. It is clearly seen that nucleation rate decreases in the presence of amino acids in the crystallization media. For each $n(L)$ function (model) and experimental data set, relative deviation was calculated. Table 4 gives the mean relative deviation values. By considering Table 4, mean relative deviation values vary between 1.025 and 1,691. It can be said that the ASL model fitted the experimental data very well.

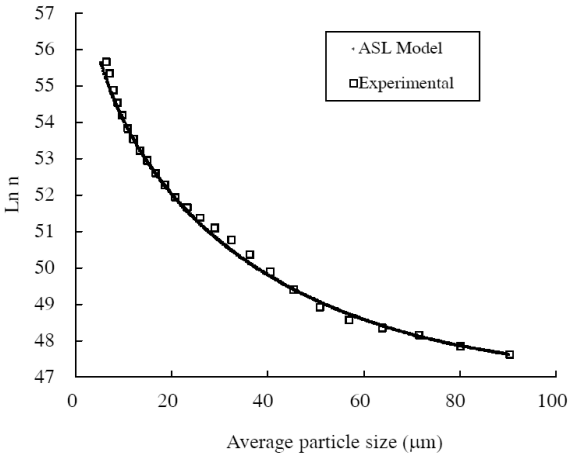

Figure 8. Size dependent analysis of the population density data according to the ASL model.

Table 3. ASL model parameters for struvite crystallization carried out in the presence of 1000 ppm amino acid concentrations for 1 h residence time.

	G^* x 10^{-8} ($m.s^{-1}$)	a x 10^4 (m^{-1})	b	n* x 10^{23} ($m^{-1}.m^{-3}$)	B* x 10^{17} ($m^{-3}.s^{-1}$)
Pure media	2,774	1,001	0,72	15,495	4,299
DL-Lysine	4,457	0,623	0,56	3,906	1,741
D(+) Proline	3,333	0,833	0,60	1,713	0,571
L-Alanine	4,486	0,619	0,57	3,690	1,655
Tryptophane	2,767	1,004	0,68	1,990	0,551

Table 4. Relative deviation values of ASL model for struvite crystallization in the presence of 1000 ppm amino acid concentrations for 1 h residence time.

	Pure Media	**DL-Lysine**	**D(+) Proline**	**L-Alanine**	**Tryptophane**
Mean Relative Deviation (%)	1,462	1,025	1,112	1,256	1,691

Crystallization experiments show that the presence of amino acids affects the struvite crystallization. As it is well known that admixtures can influence crystal growth rate in a variety of ways [21]. They may themselves be selectively adsorbed onto the crystal faces and exert a "blocking effect" or, more likely, onto the growth steps and thus disrupt the flow of growth layers across the faces. They may be built into the crystal, especially if there is some degree of lattice similarity, or they may interact chemically with the crystal and selectively alter the surface energies of the different faces. In the present study, in order to understand whether amino acids are adsorbed physically or chemically, first FT/IR analyses of struvite crystals obtained in the presence of amino acids were done. Before analyses, struvite crystals were washed by pure saturated solution three times. However, in FT/IR spectra, a peak response, the amino acid was not detected; all peaks were in agreement with FT/IR spectra of pure struvite crystals as shown in Fig. 2. This can be caused by usage of a very small amount of sample to make KBr pellets in FT/IR analyses. Thus, the presence of trace amount of adsorbed amino acid cannot be detected. So, in order to see the possible adsorption of amino acids on struvite crystals, TG/DTA analyses were also done. Fig. 9 shows the TG/DTA results of struvite crystals obtained in pure media.

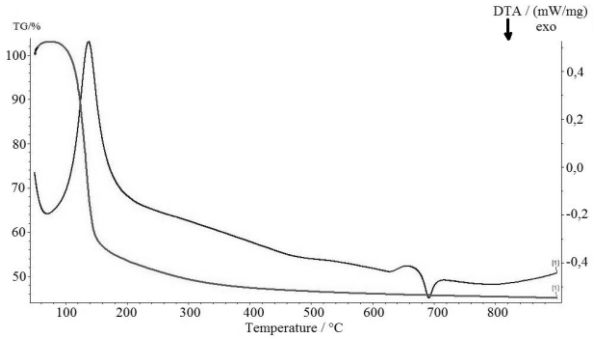

Figure 9. TG/DTA thermogram of struvite crystal grown in pure media.

In the presence of amino acids, no corresponding peaks were obtained in DTA thermogram; all peaks were in agreement with reference data for pure struvite crystals. This clearly shows that the amino acids investigated were adsorbed physically on struvite crystals. On the other hand, the kinetic and thermodynamic parameters for struvite crystals obtained both in pure media and in the presence of amino acids were reported by applying Coats and Redfern's relation to the respective thermograms of Fig. 9 [35]. This method is an integral method that assumes various orders of reaction and compares the linearity in each case to select the correct order [36]. The Coats and Redfern's relation is as follows:

$$log_{10}\left(\frac{1-(1-\alpha)^{1-n}}{T^2(1-n)}\right)=\left\{log_{10}(\frac{AR}{\alpha E})(1-\frac{2RT}{E})\right\}-\left\{\frac{E}{2.3RT}\right\} \quad (12)$$

where E is the activation energy of the reaction, A the frequency factor, α the

fraction of decomposed material at time t, n the order of reaction and T is the absolute temperature. The plots of $\left(\frac{1-(1-\alpha)^{1-n}}{T^2(1-n)}\right)$ versus $1/T$ gives straight lines for different values of n. The value of activation energy is obtained from the slope of the best linear fit plot. Fig. 10 shows an example of the Coats and Redfern plot for struvite crystals obtained in the presence of 1000 ppm tryptophane. Table 5 gives the values of activation energy E, frequency factor A and order of reaction n for struvite crystallization performed in pure media and in the presence of amino acids investigated.

Using the value of frequency factor, the values of standard entropy ($\Delta S°$) and other thermodynamic parameters such as the standard enthalpy ($\Delta H°$) and the standard Gibbs free energy ($\Delta G°$) were calculated using well-known formulae as described in literature for the dehydration stage of thermogram [37,38]. Table 6 presents the values of thermodynamic parameters for dehydration of struvite crystals obtained in pure media and in the presence of amino acids.

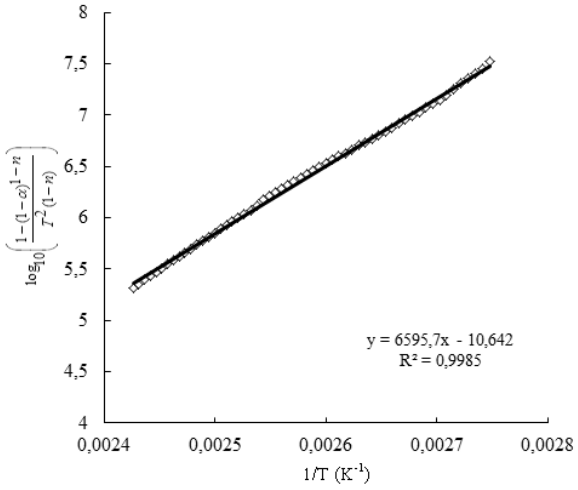

Figure 10. Graph of the Coats-Redfern method for the struvite crystals obtained in the presence of 1000 ppm tryptophane.

Table 5. Kinetic parameters obtained from TGA using the Coats Redfern Method.

	Activation Energy, E_a (kJ/mol)	**Frequency Factor, A x 10^{16} (s^{-1})**	**Reaction Order, n**	**R^2**
Pure media	123,227	0,317	1	0,997
DL-Lysine	127,962	1,330	1	0,998
D(+) Proline	126,691	0,746	1	0,999
L-Alanine	129,011	2,210	1	0,998
Tryptophane	126,289	0,704	1	0,999

Table 6. Thermodynamic parameters of struvite crystals obtained in the presence of 1000 ppm amino acid concentration for 1 h residence time.

=	**Standard Entropy, $\Delta S°$ ($J.K^{-1}.mol^{-1}$)**	**Standard Enthalpy, $\Delta H°$ ($kJ.mol^{-1}$)**	**Standard Gibbs Free Energy, $\Delta G°$ ($kJ.mol^{-1}$)**
Pure media	49,25	119,84	99,81
DL-Lysine	61,20	124,58	99,72
D(+) Proline	56,39	123,31	100,42
L-Alanine	65,49	125,66	99,25
Tryptophane	55,89	122,90	100,16

As can be seen from Table 6, all thermodynamic parameters for dehydration of struvite crystals obtained both in pure and in the presence of amino acids are positive. Here, positive value of standard enthalpy indicates that the enthalpy is increasing during the process and such process is an endhothermic process. Positive values of standard entropy, standard enthalpy and standard Gibbs free energy shows that the process is spontaneous at high temperatures.

4. Conclusions

In the presence of amino acids, struvite crystals grew in different morphologies. It was found that in all experiments a pure phase was precipitated as $MgHN_4PO_4.6H_2O$ which was confirmed by the infrared spectroscopy analysis. During the experiments struvite transformation and/or newberyite formation was not observed. The present study revealed that the presence of amino acids promoted the formation of high crystal aggregates. A possible explanation of this formation is the adsorption of the amino groups on the surface of developing crystals. Thus the growth of struvite crystals was assisted. This indicates that nutritional control of amino acids is a helpful method to prevent the formation of struvite crystals. Reduction of amino acids intake would also be expected to decrease urinary stone occurrence. The effect of amino acid on the crystallization kinetics of struvite was also presented. The calculation procedure for the ideal MSMPR crystallizer was applied; assuming both size-independent growth (ΔL McCabe's Law) and size dependent growth (modified ASL Model). Experimental results showed that growth of struvite crystals was size dependent in the absence of and in the presence of amino acids. On the basis of experimental data, using modified form of ASL Model, the following parameters: n^*, G^*, B^*, a, and b values were determined. b values were found as positive meaning growth rate increases with size-volume for all investigated conditions. The presence of amino acids in crystallization media decreased the nucleation rate in the system. This result is related to supersaturation. The kinetic and thermodynamic parameters of struvite crystals obtained at investigated experimental conditions were reported by applying Coats and Redfern equation. Standard entropy (ΔS°), standard enthalpy (ΔH°) and standard Gibbs free energy (ΔG°) were also calculated on the basis of TG/DTA studies. The values of ΔS°, ΔH° and ΔG° were positive, indicating that the the process is spontaneous at high temperatures.

Nomenclature

a, b	ASL model parameters
a (in Eq.9)	heating rate [K. min-1]
A	frequency factor [min^{-1}]
B^o	nucleation rate [$m^{-3}.s^{-1}$]
E	activation energy [J. mol^{-1}]
G	overall linear growth rate [$m^3.s^{-1}$]
G^o	growth rate of nuclei (ASL model) [m. s^{-1}]
L	crystal size [m]
n	population density [number. $m^{-1}.m^{-4}$]
n (in Eq.9)	reaction order

n^o	population density of nuclei [number. $m^{-1}.m^{-4}$]
R	ideal gas constant [J. $mol^{-1}.K^{-1}$]
t	time [s]
T	absolute temperature [K]
ΔG°	Gibbs free energy [J. mol^{-1}]
ΔH°	enthalpy [J. mol^{-1}]
ΔS°	entropy [J. $mol^{-1}K^{-1}$]

Greek Letters

α	the fraction of decomposed material at time t.
τ	residence time [s]

References

[1] Lee, S.I., Weon, S.Y., Lee, C.W. and Koopman, B., "Removal of nitrogen and phosphate from wastewater by addition of bittern", Chemosphere, 51, 265, (2003).

[2] Doyle, J.D. and Parsons, S.A., "Struvite formation control and recovery", Water Res., 6, 3925, (2002).

[3] Ariyanto, E., Kanti Sen, T. and Ming Ang, H., "The influence of various physic-chemical process parameters on kinetics and growth mechanism of struvite crystallization", Adv. Powder Technol., 25, 682, (2014).

[4] Le Corre, K.S., Valsami-Jones, E., Hobbs, P. and Parsons, S.A., "Impact of calcium on struvite crystal size, shape and purity", J. Cryst. Growth, 283, 514, (2005).

[5] Deng, S.P. and Ouyang, J.M., "Effects of dipalmitoylphosphatidylcholine monolayers to the crystallization of calcium oxalate monohydrate from the solution containing chondroitin sulfate C", Colloids and Surfaces, A: Physicochemical and Engineering Aspects, 257, 47, (2005).

[6] Ouyang, J.M. and Deng, S.P., "Controlled and uncontrolled crystallization of calcium oxalate monohydrate in the presence of citric acid", Dalton Trans., 14, 2846, (2003).

[7] Wang, L., Zhang, W., Qiu, S.R., Zachowicz, W.J., Guan, X., Tang, R., Hoyer, J.R., De Yoreo, J.J. and Nancollas, G.H., "Inhibition of calcium oxalate monohydrate crystallization by the combination of citrate and osteopontin", J. Cryst. Growth, 291 (1), 160, (2006).

[8] Ouyang, J.M., Deng, S.P., Zhong, J.P., Tieke, B. and Yu, S.H., "Crystallization of calcium oxalate monohydrate at dipalmitoylphosphatidylcholine monolayers in the presence of chondroitin sulfate A", J. Cryst. Growth, 270(3-4), 646, (2004).

[9] Creighton, T.E., Proteins: Structure and molecular properties, 2nd ed., WH Freeman, New York, (1993).

[10] Sakami, W. and Harrington, H. "Amino acid metabolism", Annual Review of Biochemistry, 32, 355, (1963).

[11] Young, V.R., "Adult amino acid requirements: The case for a major revision in current recommendations", J. Nutr., 124 (8), 1517, (1994).

[12] Ferreira, L.A., Macedo, E.A. and Pinho, S.P., "Solubility of amino acids and diglycine in aqueous–alkanol solutions", Chem. Eng. Sci., 59(15), 3117, (2004).

[13] Moorthy Babu, S., Geetha, S.K., Perumal, R. and Anbarasan, P.M., "Habit modification and improvement in properties of potassium hydrogen

phthalate (KAP) crystals doped with metal ions", Cryst. Res. Technol., 41, 221, (2006).

[14] Ramesh Babu, R., Vijayan, N., Gopalakrishnan, R. and Ramasamy, P., "Growth and characterization of L-lysine monohydrochloride dehydrate (L-LMHCl) single crystal", Cryst. Res. Technol., 41, 405, (2006).

[15] Koutsopoulos, S. and Dalas, E., "The effect of acidic amino acids on hydroxyapatite crystallization", J. Cryst. Growth, 217, 410, (2000).

[16] Chuajiw, W., Takatori, K., Igarashi, T. and Hara, H., "The influence of aliphatic amines, diamines and amino acids on the polymorph of calcium carbonate precipitated by the introduction of carbon dioxide gas into calcium hydroxide aqueous suspensions", J. Cryst. Growth, 386, 119, (2014).

[17] Sugihara, H., Ono, K., Adachi, K., Setoguchi, Y., Ishihara, T. and Takita, Y., "Synthesis of disk-like calcium carbonate (part 1) ", J. Ceram. Soc. Jpn., 104, 832, (1996).

[18] Sugihara, H., Anan, T., Adachi, K., Baba, A., Egashira, N. and Nishiguchi, H., "Synthesis of disk-like calcium carbonate (part 2) ", J. Ceram. Soc. Jpn., 105, 886, (1997).

[19] Lakshminarayanan, R., Valiyaveettil, S. and Loy, G.L., "Selective nucleation of calcium carbonate polymorphs: Role of surface functionalization and poly (vinyl alcohol) additive", Cryst. Growth Des., 3, 953, (2003).

[20] Wang, W., Wang, G., Liu, Y., Zheng, C. and Zhan, Y., "Synthesis and characterization of aragonite whiskers by a novel and simple route", J. Matter. Chem., 11, 1752, (2001).

[21] Mullin, J.W., Crystallization, 4th ed., Elsevier, Butterworth-Heinemann, (2001).

[22] Sargut, S.T., Sayan, P. and Kiran, B., "Influence of essential and non-essential amino acids on calcium oxalate crystallization", Cryst. Res. Technol., 45 (1), 31, (2010).

[23] Holdich, R.G., "Rotary vacuum filter scale-up calculations and the use of computer spreadsheets", Filtr Separat., 27 (6), 435, (1990).

[24] Stevof, V., Soptrajanov, B., Spirovski, F., Kuzmanovski, I., Lutz, H.D. and Engelen, B., "Infrared and raman spectra of magnesium ammonium phosphate hexahydrate (struvite) and its isomorphous analogues", J. Mol. Struct., 752, 60, (2005).

[25] Bemrose, C.R. and Bridgwater J., "A review of attrition and attrition test methods", Powder Technology, 49, 97, (1987).

[26] Randolph, A.D., Larson, M.A., Theory of particulate processes: Analysis and techniques of continuous crystal-lization, Academic press, New York, (1988).

[27] Garside, J., Mersmann, A. and Nyvlt, J., Measurement of crystal growth rates, 1st ed., European Federation of Chemical Engineering, Working Party on Crystallization, (1990).

[28] Koralewska, J., Piotrowski, K., Wierzbowska, B. and Matynia, A., "Kinetics of reaction– crystallization of struvite in the continuous draft tube magma type crystallizers – influence of different internal hydrodynamics",

Chinese J., Chem. Eng., 17(2), 330, (2009).

[29] Bransom, S.H., "Factors in the design of continuous crystallizers", Brit. Chem. Eng., 5, 838, (1960).

[30] Mydlarz, J. and Jones, A.G., "On modeling the size dependent growth rate of potassium sulphate in a MSMPR crystallizer", Chem. Eng. Comm., 90, 47, (1990).

[31] Mydlarz, J., "A hyperbolic crystal growth rate model", Proceedings of 13th Symposium on Industrial Crystal-lization, Toulouse, France, pp. 275-280, (1996).

[32] Abegg, C.F., Stevens, J.D. and Larson, M.A., "Crystal size distribution in continuous crystallizers when growth rate is size dependent", AIChE J. , 14, 118, (1968).

[33] Abegg, C.F., Stevens, J.D. and Larson, M.A., "Crystal size distributions in continuous crystallizers when growth rate is size dependent", AIChE J., 14, 118, (1968).

[34] Garside, J. and Jancic, S.J., "Growth and dissolution of potassium-alum crystals in the subsieve size range", AIChE J., 22, 887, (1976).

[35] Coats, A.W. and Redfern, J.P., "Kinetic parameters from thermogravimetric data", Nature, 201, 68, (1964).

[36] Tonbul, Y. and Yurdakoç, K., "Thermogravimetric investigation of the dehydration kinetics of KSF, K10 and Turkish bentonite", Turk J. Chem., 25, 333, (2001).

[37] Joshi, V.S. and Joshi, M.J., "FTIR spectroscopic, thermal and growth morphological studies of calcium hydrogen phosphate dihydrate crystals", Cryst. Res. Technol., 38 (9), 817, (2003).

[38] Laidler, K.J. Chemical Kinetics, 3rd ed., Harper and Row, New York, (1987).